

Investigation of Excited State Intramolecular Proton Transfer and Structural Dynamics in Bis-benzimidazole Derivative (BBM) Using Femtosecond Stimulated Raman Spectroscopy

[Junhan Xie](#), Ziyu Wang, [Ruixue Zhu](#), Jiaming Jiang, [Tsu-Chien Weng](#), Yi Ren, Shuhua Han, [Yifan Huang](#)^{*}, [Weimin Liu](#)^{*}

Posted Date: 25 April 2023

doi: 10.20944/preprints202304.0894.v1

Keywords: excited state intramolecular proton transfer; structural dynamics; transient absorption; femtosecond fluorescence up-conversion; femtosecond stimulated Raman spectroscopy



Preprints.org is a free multidiscipline platform providing preprint service that is dedicated to making early versions of research outputs permanently available and citable. Preprints posted at Preprints.org appear in Web of Science, Crossref, Google Scholar, Scilit, Europe PMC.

Copyright: This is an open access article distributed under the Creative Commons Attribution License which permits unrestricted use, distribution, and reproduction in any medium, provided the original work is properly cited.

Article

Investigation of Excited State Intramolecular Proton Transfer and Structural Dynamics in Bis-Benzimidazole Derivative (BBM) Using Femtosecond Stimulated Raman Spectroscopy

Junhan Xie ¹, Ziyu Wang ¹, Ruixue Zhu ¹, Jiaming Jiang ¹, Tsu-Chien Weng ¹, Yi Ren ¹, Shuhua Han ², Yifan Huang ^{1,*} and Weimin Liu ^{1,3,*}

¹ School of Physical Science and Technology, ShanghaiTech University, Shanghai 201210, China

² Key Lab of Colloid and Interface Chemistry, Ministry of Education, Shandong University, Jinan 250100, China

³ STU and SIOM Joint Laboratory for Superintense Lasers and the Applications, Shanghai 201210, China

* Correspondence: huangyf@shanghaitech.edu.cn (Y.H.); liuwm@shanghaitech.edu.cn (W.L.)

Abstract: Bis-benzimidazole derivative (BBM) molecule, consisting of two 2-(2'-Hydroxyphenyl) benzimidazole (HBI) halves, has been synthesized and successfully utilized as a ratiometric fluorescence sensor for the sensitive detection of Cu²⁺ based on enol-keto excited state intramolecular proton transfer (ESIPT). In this study, we strategically implement femtosecond stimulated Raman spectroscopy and several time-resolved electronic spectroscopies, aided by quantum chemical calculations to investigate the detailed primary photodynamics of BBM molecule. The results demonstrate that the ESIPT from BBM-enol* to BBM-keto* was observed in only one of HBI halves with a time constant of 300 fs, after that, the rotation of the dihedral angle between two HBI halves generate a planarized BBM-keto* isomer in 3 ps, leading to dynamics red shift of BBM-keto* emission.

Keywords: excited state intramolecular proton transfer; structural dynamics; transient absorption; femtosecond fluorescence up-conversion; femtosecond stimulated Raman spectroscopy

1. Introduction

Derivatives of 2-(2'-hydroxyphenyl) benzimidazole (HBI) and its analogs 2-(2'-hydroxyphenyl) benzoxazole (HBO) and 2-(2'-hydroxyphenyl) benzothiazole (HBT) have been widely used for metal ions Zn²⁺ and Cu²⁺ selective emission ratiometric probe, due to large stokes shift and dual fluorescence emission based on enol → keto excited state intramolecular proton transfer (ESIPT) [1–5]. As molecules binding to the metal cations are highly sufficient, the metal cations as ligands can disrupt the ESIPT process, which leads to diminishing keto emission and simultaneously enhances the enol fluorescence emission [1]. It has been demonstrated that the ESIPT processes of hydrogen bonding molecules having a hydroxyl group as a proton donor, such as HBT [6–9], HBO [10,11], HBI [12,13] are usually highly exergonic with a low barrier or barrierless, leading to remarkably ultrafast proton transfer. Despite such a unique application, the efficiency of the large stokes shift keto emission is generally low due to *cis* to *trans* photoisomerization via the C=C bond between the benzene ring and five-membered heterocycles [9], which significantly affects the detection effect of the proportional fluorescent probe. An in-depth understanding of the photophysics of these kinds of molecules is critical to determining the underlying mechanisms for successful metal ions probes in cell biology. The behaviors of ESIPT and photoisomerization have been investigated by time-resolved spectroscopies, including fluorescence upconversion measurements and broadband femtosecond transient absorption spectroscopy [9,14–17]. These photophysical studies indicate solvent-dependent

ESIPT rates varying ranged from a hundred femtoseconds to a few picoseconds [9,14,18]. However, the details of the photoisomerization of those molecules are still not well understood. By using Raman loss femtosecond stimulated Raman technique, *Umapathy et al.* demonstrated direct evidence for the involvement of torsional motion leading to an ultrashort lifetime of HBT which indicates the evolution of the planar cis-keto* form to the twisted keto* form [19].

In this study, we combined tunable femtosecond stimulated Raman spectroscopy (FSRS) [20–25], transient absorption (TA), and fs fluorescence upconversion spectroscopy to comprehensively elucidate the ESIPT and conformational change of bis-benzimidazole derivative (BBM) molecule which consists two HBI-derivative (see Figure 1) and has been successfully used as a ratiometric fluorescence sensor for the sensitive detection of Cu^{2+} [26]. Different from the HBI molecule, BBM exhibits unique ESIPT and intramolecular twisting dynamics, of which the ESIPT was observed in only one of HBI halves in BBM molecule to form BBM-keto* with a time constant of 300 fs, after that, instead of the *cis* to *trans* photoisomerization via C14-C15 (or C23-C25) bond, the rotation of the dihedral angle between two HBI halves pivoted on the C7-C4 generate a planarized BBM-keto* isomer and lead to a dynamic Stokes shift of BBM-keto* fluorescence emission.

2. Results and Discussion

2.1. Steady-State Absorption and Fluorescence Spectroscopy

The normalized absorption and emission spectra of BBM in tetrahydrofuran -THF (relative polarity: 0.2; viscosity: 0.55 cP) and Dimethyl sulfoxide -DMSO (relative polarity: 0.44; viscosity: 2.24 cP). are presented in Figure 1a. The absorption band of BBM is observed at ~ 350 nm in both solvents and is ascribed to the π - π^* transition between benzimidazole and hydroxypheny. Two maxima at 340 and 350 nm are assigned to the anti-enol and cis-enol BBM conformers, respectively [27,28]. The BBM fluorescence spectra exhibit a significant Stokes shift of 86 nm in THF and 95 nm in DMSO versus the absorption peak, indicating keto emission after ESIPT. Furthermore, a weak shoulder at 390 nm was observed, which is attributed to fluorescence emission of the BBM-enol* form (see Figure S1). The bathochromic spectral shift of the keto emission with respect to the polar solvents can be interpreted as the effect of solvent polarity on the excited electron states BBM-keto*.

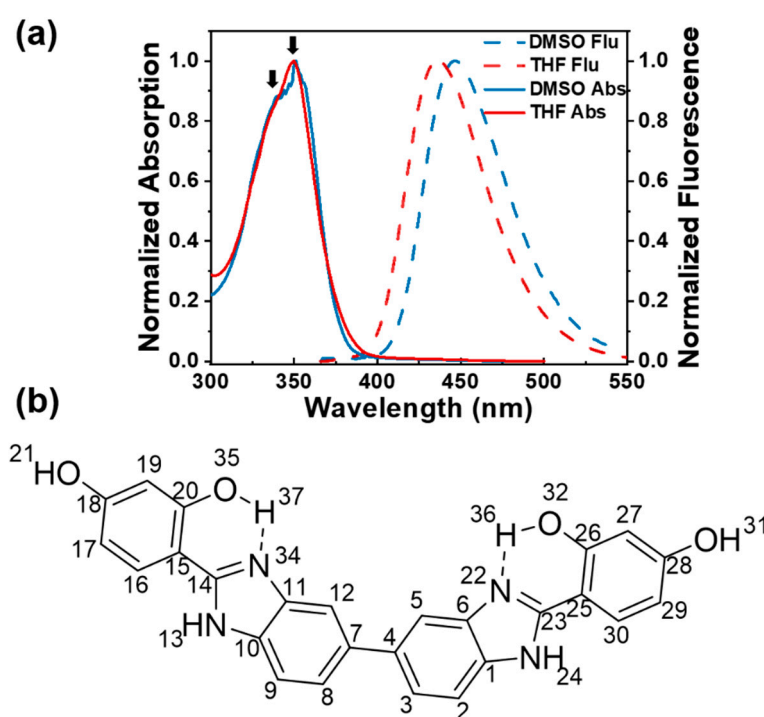


Figure 1. (a) Steady-state absorption and fluorescence spectra of BBM in DMSO and THF; (b) Molecular structure of BBM-enol form.

2.2. Femtosecond Transient Absorption Spectroscopy

Femtosecond transient absorption (TA) measurements were first performed to obtain the excited state dynamics of BBM molecule. Figure 2a and S2a show ultrafast two-dimensional TA spectra of BBM molecules in DMSO and THF under excitation at 350 nm with a power intensity of 70 nJ/pulse. The TA spectrum against the delay time from -1 ps to 8 ns exhibits intricate excited state features between 350 nm and 650 nm including three excited state absorption bands (ESA1 band center at 380 nm; ESA2 band center at 440 nm; ESA3 band of 460 nm - 640 nm), the stimulated emission band (SE center at 450 nm) and the ground-state bleach at the blue edge. Moreover, global analysis with a parallel model was employed to obtain the decay-associated difference spectra (DADS, see Figure 2b), yielding four characteristic lifetimes with time constants of $\tau_1 = 0.3$ ps, $\tau_2 = 3.0$ ps, $\tau_3 = 1.6$ ns, and $\tau_4 =$ infinitely long lifetime in DMSO.

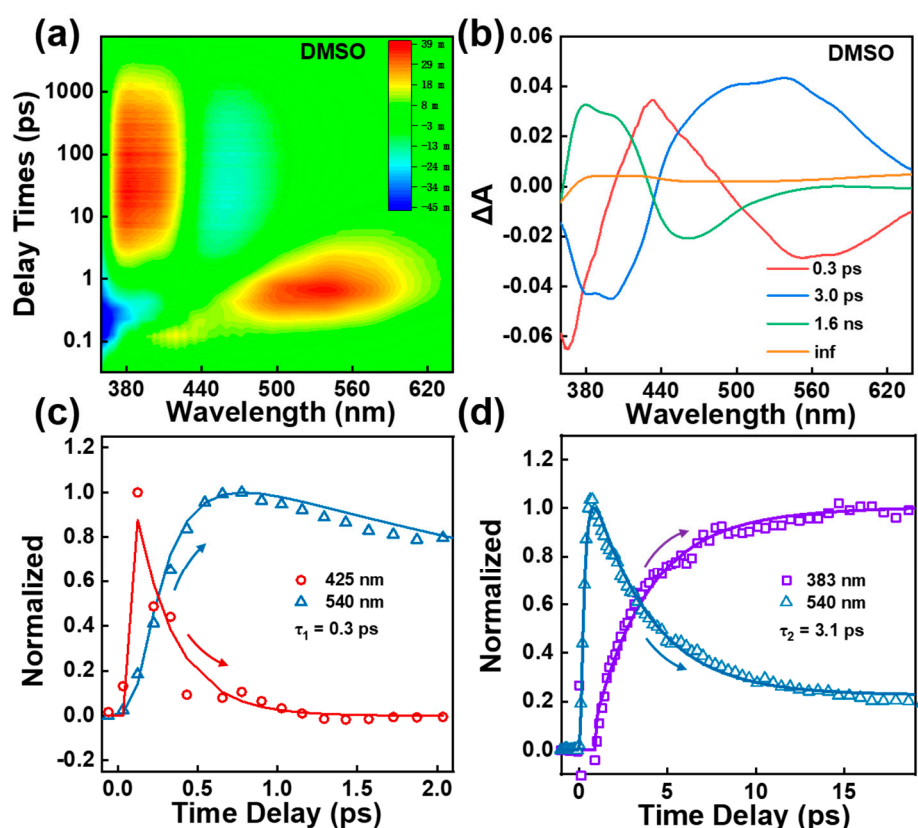


Figure 2. (a) 2D plot of TA spectrum of BBM in DMSO at 350 nm excitation; (b) Decay-associated difference spectra (DADS) of TA spectrum of BBM in DMSO; (c) Transient amplitude of the TA spectra of BBM probe at 425 nm and 540 nm in DMSO; (d) Transient amplitude of the TA spectra of BBM probe at 383 nm and 540 nm in DMSO.

As shown in Figure S3, between the 0 and 0.6 ps time scales, the BBM temporal trace in DMSO at 425 nm (ESA 2 band) exhibits initial rapid decay dynamics with a time constant of 0.3 ps, and the ESA 3 band at 540 nm rise significantly on the same timescale (see Figure 2c). This evolution is attributed to the ESIPT from the excited state of BBM-enol* to BBM-keto*. After 0.6 ps, as shown in Figure 2d, the ESA3 band at 540 nm exhibits a dominant two exponential decay with time constants of $\tau_2 = 3.1$ ps and $\tau_4 =$ infinitely long lifetime. Notably, the decay of the ESA3 band is followed by the increase of ESA 1 band signal at 383 nm in 3.1 ps (see Figure 2d). The ESA 1 band at 383 nm then decays with two exponential processes of $\tau_3 = 1.6$ ns, and $\tau_4 =$ infinitely long lifetime (see Figure S4). The SE band at 450 nm reveals 1.6 ns decay dynamics indicating that the 1.6 ns is attributed to the spontaneous emission lifetime from the excited state of BBM-keto*, which was further confirmed

using the fs up-conversion fluorescence spectroscopy at an excitation of 350 nm, as shown in Figure 3. We utilized EOS-TA measurements in the ns \sim μ s time range to determine the longest-lived components τ_4 in TA spectra. As shown in Figure S5a,c in the Supplementary Material, a broad ESA band in the range of 370 - 850 nm exhibits single exponential decay with a time constant of 66 ns, indicating depopulation from BBM-keto triplet state T_1 state [9,29].

The previous reports have demonstrated that the significant role of twisting motion pivot on C23-C25 (C14-C15) bond was observed from the HBI-keto*, which results in fluorescence quenching via cis-trans photoisomerization [6,9,30]. To probe possible photoisomerization of BBM in the course of the primary photo-processes, the sample was measured in THF with low viscosity using TA. As shown in Figure S2b, the DADS of BBM in THF reveal four exponential decay components of 0.3 ps (τ_1), 2.6 ps (τ_2), 1.7 ns (τ_3) and an infinite lifetime (τ_4), the longest τ_4 time components are well resolved with a time constant of 862 ns, which is assigned to the triplet keto- T_1 state lifetime (see Figure S5b,d). The spectral shape of each DADS component does not show differ from that in DMSO solvent, indicating that the intermediate states of the BBM molecule remain unchanged in THF (see Figure 2b and Figure S2b). Notably, the second component τ_2 has shorter lifetimes in the low viscous THF solvent versus that in DMSO, indicating that a conformational change occurs after ESIPT processes.

2.3. Femtosecond Fluorescence Up-Conversion Spectroscopy

Our TA spectra thus far suggest enol to keto ESIPT which is followed by the photoinduced conformational change of BBM chromophore. However, two open questions here remain unclear. First, is the conformational change caused by the C23-C25 and/or C14-C15 bond cis-trans photoisomerization or other types of distortion? Second, does the ESIPT occur at both HBI halves of BBM molecule? To address the first question, we obtained time-resolved up-conversion fluorescence spectra for BBM following 350 nm excitation (see Figure 3 and S6). As shown in Figure 3a, in DMSO, a blue emission band maximize at approximately 438 nm at time zero, as time elapsed, the emission band redshifts to a final position nearly corresponding to the steady-state emission spectrum with a maximum of 445 nm. The DADS spectra yield three components including $\tau_1 = 0.3$ ps rising dynamics followed by $\tau_2 = 2.9$ ps, and $\tau_3 = 1.3$ ns (see Figure 3b). The ultrafast rise with a time of 0.3 ps reflects the formation of the BBM-keto* component via the ESIPT. In particular, the transient intensity of emission on the blue side of the emission band (420 nm) exhibits an ultrafast rise (~ 0.3 ps) followed by a dominant fast decay component of 2.7 ps and a long decay lifetime of 1.3 ns (see Figure 3c); at the longest emission wavelength of 480 nm, the kinetics is well fitted by a fast rise of 2.7 ps and a 1.3 ns single exponential decay components, in which the rise of 2.7 ps matches the decay component of the short emission wavelength at 420 nm and is consistent with the τ_2 component obtained from TA spectra. In THF solvent, as shown in Figure S6b, similar excited-state features were observed as DMSO, three components of $\tau_1 = 0.3$ ps, $\tau_2 = 1.6$ ps, and $\tau_3 = 1.2$ ns were required for best fit.

The transient amplitude and frequency change of the second component τ_2 in two solvents show distinct dynamics differences (see Figure 3c, S7 and S8). Note that the solvent relaxation time of DMSO and THF is 1.8 ps and 0.9 ps, respectively [31], in both solvents, as shown in Figure S8 the prolonged transient dynamic stokes shift (3.9 ps in DMSO; 1.5 ps in THF) indicate that solvation and conformational change might occur simultaneously until the system is completely solvated, and that afterward, conformational change dynamics primarily control the excited state relaxation [21,32]. Additionally, the DADS spectrum of τ_2 displays a dispersive lineshape indicating a dynamic redshift with enhanced fluorescence intensity (see Figure 3d). This phenomenon cannot be attributed to cis-trans photoisomerization along C23-C25 or C14-C15 bonds in BBM-keto* form, as such photoisomerization would effectively quench fluorescence intensity and result in non-radiative decay. [6,9]. There is, however, a flexible point at the C4-C7 central bridge which may facilitate conformational changes by rotating the dihedral angle between two HBI halves of BBM-keto* form [33–36].

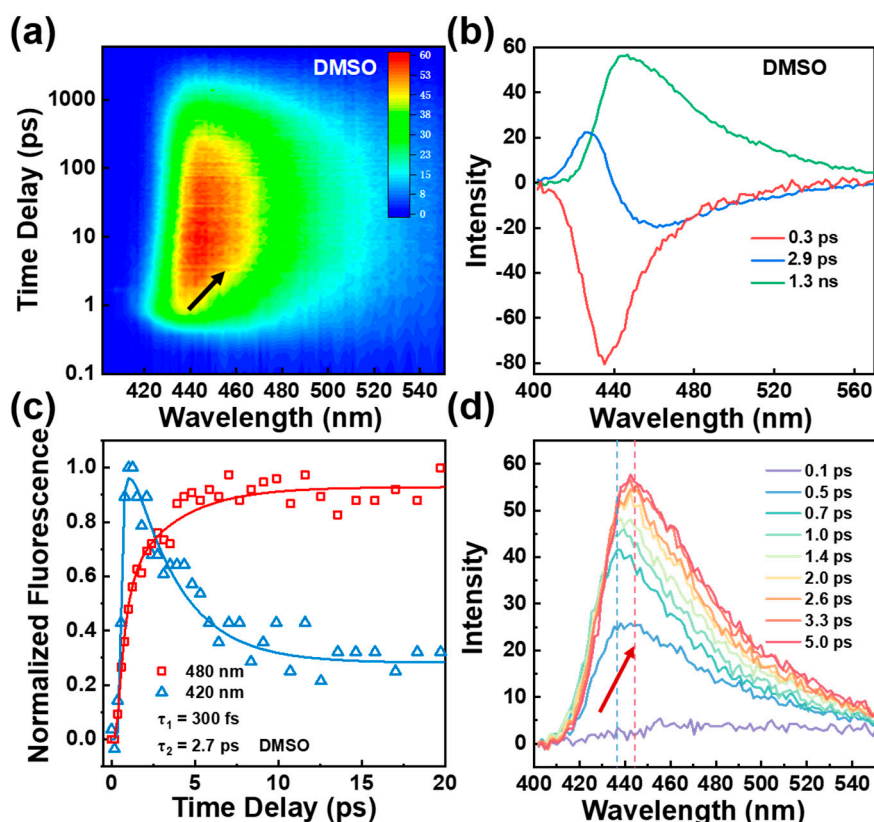


Figure 3. (a) 2D plot of fs fluorescence up-conversion spectra of BBM under 350 nm excitation in DMSO; (b) DADS spectrum of fs fluorescence up-conversion of BBM in DMSO; (c) Transient amplitude of BBM fluorescence probe at 420 nm and 480 nm in DMSO; (d) fs fluorescence up-conversion spectra of BBM in DMSO at different delay times.

2.4. Femtosecond Raman Stimulated Spectroscopy

To summarize our findings thus far, the TA experimental and upconversion fluorescence results provide evidence for ESIPT and conformational change evolution in the BBM molecule. However, further support is required to precisely assign the τ_1 and τ_2 time constants. For τ_1 , does the ESIPT occur at two HBI halves or only one of the HBI half in BBM? For τ_2 , does the conformational change derived from the rotation through C₄-C₇ bond? To gain more experimental insights into conformational change during ESIPT, FSRS was used to track local vibrational marker bands on the excited states [20–22,24,25,37,38]. We strategically selected 600 and 480 nm Raman pump, which correspond to the red shoulder of BBM-keto* and BBM-enol* ESA bands. This pre-resonantly enhances the FSRS signal on the Stokes side (see Figure S10), providing the excited-state Raman signals that reveal intricate dynamics tracking ESIPT and the structural change of BBM molecules [20–22]. Figure 4a reveals a 2D contour plot of FSRS spectra for BBM across the frequency range of 850 cm⁻¹ - 1700 cm⁻¹ in DMSO with Raman pump excitation of 600 and 480 nm (baseline drawn and FSRS raw data are shown in Figure S9 in supplementary material). Five excited-state Raman peaks were observed at 953 cm⁻¹(I), 1130 cm⁻¹(II), 1358 cm⁻¹(III), 1565 cm⁻¹(IV), and 1587 cm⁻¹(V) under the Raman pump excitation of 480 nm (BBM-enol* form). A more detailed description of Raman modes at BBM-enol form was achieved through density functional theory (DFT) with the optimized geometry at the dihedral angles between two HBI halves at $\Theta = 39^\circ$ and between benzene and imidazole rings at $\Phi = 0^\circ$. As illustrated in Figure S11 and Table S1, the observed Raman modes at 1565 cm⁻¹, and 1587 cm⁻¹ are mainly attributed to the C14-C15 (C23-C25) stretching accompanied by the benzene and imidazole rings deformation; the mode at 1358 cm⁻¹ is assigned to the benzene and imidazole rings stretching and C-H in-plane wagging; 1130 cm⁻¹ is attributed to C-H in-plane wagging motions of two benzene rings; 953 cm⁻¹ is attributed to C-H out-of-plane bending of two benzene

rings. Those modes shift to 939 cm^{-1} (I), 1122 cm^{-1} (II), 1348 cm^{-1} (III), 1534 cm^{-1} (IV), and 1568 cm^{-1} (V) at the Raman pump of 600 nm (BBM-keto* form).

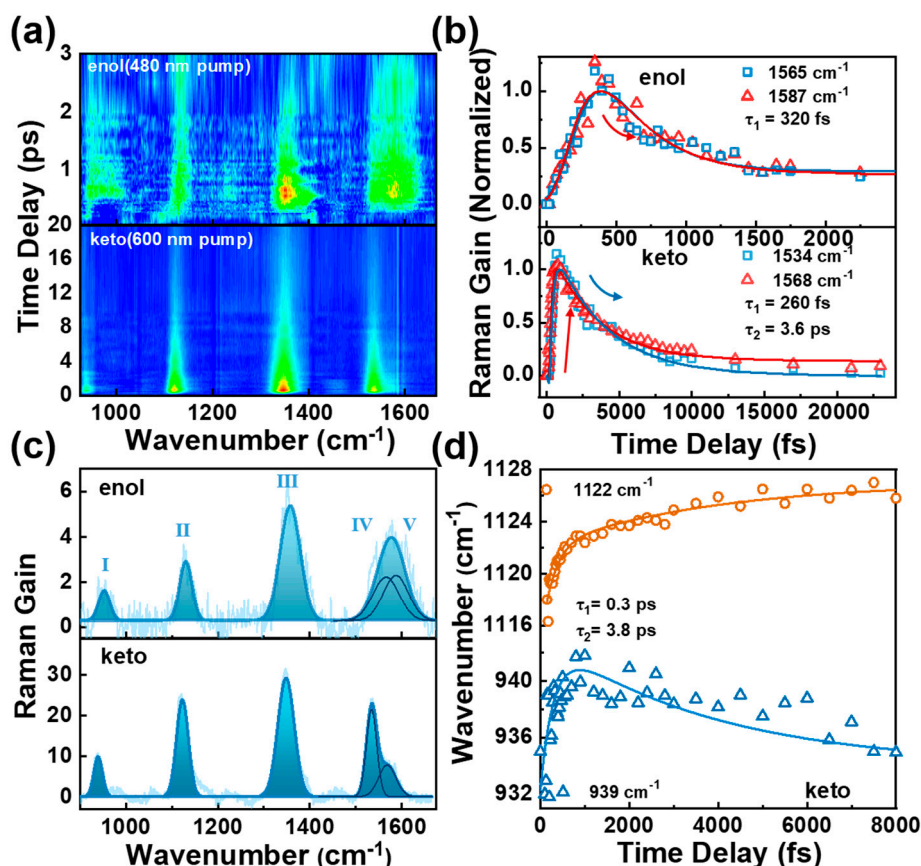


Figure 4. (a) FSRs 2D plot of BBM stimulated by 350 nm, resonantly enhanced by 480 nm and 600 nm in DMSO; (b) Transient amplitude of Raman modes (IV) and (V) with 480 nm and 600 nm Raman Pump; (c) FSRs spectra of BBM-enol* and of BBM-keto* forms; (d) Transient frequency of the Raman modes (I) and (II) of BBM-keto* in DMSO.

Figure 4b presents the transient amplitude of Raman modes (IV) and (V) of BBM in DMSO at different Raman pump wavelengths. Upon the excitation with a 480 nm Raman pump, both Raman modes exhibit two exponential decays with a time constant of $\tau_1 = 320\text{ fs}$ and an infinite long lifetime. The τ_1 is consistent with the ESIPT rate observed in TA and up-conversion fluorescence, indicating resonantly enhances excited state Raman signal of BBM-enol* form under the excitation of 480 nm Raman pump; the subsequent infinite long lifetime can be attributed to the decay of fluorescence emission from BBM-enol* state. By using 600 nm Raman pump, the transient amplitude of these two Raman modes exhibits a rising dynamics of $\tau_1 = 260\text{ fs}$ followed by two exponential decays with time constants of $\tau_2 = 3.6\text{ ps}$ and an infinite long lifetime. Moreover, Figure S12 illustrates that τ_2 displays significant viscosity-dependent dynamics in THF (2.6 ps) and corroborates the aforementioned conformational change dynamics observed in TA and fs up-conversion spectra. Importantly, as shown in Figure 4c, the difference in peak frequency between modes (IV) and (V) is 22 cm^{-1} in BBM-enol* form (with Raman pump of 480 nm), which increases to 34 cm^{-1} in BBM-keto* form (with Raman pump of 600 nm). As presented in Table S1, the DFT calculations demonstrate a slight decrease in the peak frequency difference of the two Raman modes from BBM-enol (4 cm^{-1}) to BBM-keto (3 cm^{-1}) when the ESIPT occurs in both HBI halves. Conversely, if the ESIPT only takes place in one HBI half of BBM, there is a significant increase in the peak frequency difference from 4 cm^{-1} in BBM-enol* form to 38 cm^{-1} in BBM-keto* form, which aligns with the experimental observation. Additionally, Figure 4c demonstrates that the FSRs spectra at 480 nm Raman pump excitation exhibit equal peak intensity

for the two Raman modes (IV) and (V) with Gaussian line shape in the BBM-enol* form. However, in the BBM-keto* form (600 nm Raman pump), there is a difference in peak intensity between these two Raman modes due to ESIPT occurring in one HBI half of BBM, resulting in different Raman polarizability.

Figure 4d illustrates the transient frequency shift of mode (I) and (II) in BBM-keto* form with Raman pump excitation of 600 nm. The 934 cm⁻¹ mode rapidly blueshifts to 941 cm⁻¹ in 0.3 ps, followed by a slow redshift to 936 cm⁻¹ with time constants of 3.8 ps; while mode (II) exhibits two exponential frequency blueshifts from 1117 cm⁻¹ to 1128 cm⁻¹ with time constants of 0.3 ps and 3.8 ps. The initial blueshift of the two Raman modes can be attributed to the vibrational cooling process accompanied by ESIPT. To investigate the second transient frequency change in those modes, TD-DFT calculations were performed for the BBM-keto* form with ESIPT occurring in one HBI half of BBM. The optimized geometry at the S1 electronic excited state of BBM-keto* reveals the dihedral angle of $\Theta = 26^\circ$ and $\Phi = \sim 0^\circ$. By reducing the Θ from 39° (the dihedral angle on S1 Franck-Condon state) to 26° while keeping the $\Phi = 0^\circ$, it was observed that the Raman modes (I) and (II) exhibit red shift and blue shift, respectively, during the twisting of Θ (see Figure S13). This suggests that the second transient frequency change is caused by rotation of the dihedral angle Θ between two halves of BBM, ultimately leading to a planarized BBM-keto* isomer.

At last, to clarify the electron transitions responsible for the dynamic red shift fluorescence spectra observed in fs fluorescence up-conversion spectra, we used TD-DFT to calculate the energy gap and the oscillator strength of the S1 \rightarrow S0 transition of BBM-keto* form (ESIPT occurs in one HBI half of BBM) at different torsion angles $\Theta = 26^\circ$, 30° , and 35° in the S1 excited state. The results presented in Table S2 demonstrate an evident fluorescence spectral redshift and an increase in oscillator strength as the Θ is tuned from 39° to 26°. This finding is consistent with the experimental observation of fs fluorescence up-conversion spectra, further confirming that the planarization via Θ dihedral angle torsion plays a crucial role in the excited state relaxation of BBM keto* state.

3. Materials and Methods

3.1. Synthesis of BBM

As shown in Scheme. S1 in support information. NaHSO₃ (0.97 g, 9.33 mmol) and 2,4-Dimethylbenzaldehyde (1.29 g, 9.33 mmol) were dissolved in 50 mL ethanol. And the resultant mixture was stirred at room temperature for 12 h. A DMF solution (50 mL) containing 3,3-Diaminobenzidine (1 g, 4.67 mmol) was then added, and the mixture was continuously stirred under reflux for 12 h at 80°C. After cooling to room temperature, vacuum distillation was available to remove most of the solvents and the precipitate was obtained by adding 100 mL of deionized water. The compound was collected by filtration and washed with deionized water. The resulting solid was dried for 3 days to afford the production with a yield of 71%.

3.2. Transient Absorption Spectroscopy

Transient absorption (TA) spectroscopy was carried out on commercial transient absorption (HELIOS, Ultrafast System). The 800 nm laser pulse was generated from a commercial mode-locked Ti: sapphire laser (Coherent, Astralla tunable USP, 35 fs, 7 mJ/pulse, 1 kHz repetition rate). A 350 nm pulse was used as the actinic pump to stimulate the sample at TA experiment, which was generated by 800 nm laser passing an optical parametric amplifier. (OPerA solo, Coherent Inc), the pulse duration of the output from OPA is about 60 fs. A white light continuum ranging from ~ 350 nm to ~ 650 nm serves as the probe pulse, which was obtained by focusing on a 2 mm-thick sapphire. The instrument response function (IRF) of this TA system was determined to be 120 fs.

EOS-TA spectroscopy was carried out on commercial transient absorption (HELIOS, Ultrafast System). A 350 nm pulse generated by 800nm light source passing an optical parametric amplifier (OPerA solo, Coherent Inc) was used as the actinic pump. A broadband supercontinuum white light with a wavelength range from ~ 350 nm to ~ 800 nm serves as the probe pulse, which was generated through a sub ns white light laser.

3.3. Time-Resolved Up-Conversion Fluorescence Spectroscopy

The fs fluorescence upconversion spectroscopic measurements were performed using a commercial time-resolved fluorescence upconversion spectrometer (Halcyone Fire, Ultrafast Systems LLC). The excited wavelength of fluorescence upconversion experiments was selected at 350 nm as actinic pump. The gate pulse comes from a small portion of an 800 nm fundamental beam. The fluorescence generated by the sample is collected and interacts with the gate pulse to produce a sum frequency signal on the BBO crystal. Upconversion signals were gathered using a monochromator and detected using a CCD camera. The time resolution was determined to be ~250 fs.

3.4. Femtosecond Stimulated Raman Spectroscopy (FSRS)

The fundamental laser pulses (Astrella, Coherent, Inc, 35 fs pulse duration, 7 mJ pulse energy, and 1 kHz repetition rate) were split into three beams to generate a tunable narrowband picosecond (ps) Raman pump, a broadband femtosecond (fs) Raman probe, and an fs actinic pump. The actinic pump beams centered at 350 were generated by an optical parametric amplifier/OPA (OPerA Solo, Coherent, Inc.) for excited-state FSRS. About 3 W of fundamental pulses was directed through a second harmonic bandwidth compressor (SHBC, Coherent, Inc.) and a ps-OPA system (TOPAS-400, Coherent, Inc.) to generate a ps pulses as the Raman pump (300 nJ pulse energy). About 15 mW of the fundamental laser output was focused onto a 2-mm-thick single-crystal sapphire plate to obtain the supercontinuum white light as Raman probe. The instrument response time was measured by cross correlation between the fs actinic pump and Raman probe pulses to be ~150 fs.

3.5. Calculations

Density functional theory (DFT) and time-dependent DFT (TD-DFT) computations were carried out at the level of PBE1PBE/6-311+G** by using Gaussian 09 package. (cite: Gaussian 09, Revision E.01, M. J. Frisch, et al. Gaussian, Inc., Wallingford CT, 2013.) The ground state and excited states were geometrically optimized. Vibrational frequencies were calculated on the optimized geometries. The solvation effect was described by the polarizable continuum model (PCM) [39–44].

4. Conclusions

In this study, we exploit several ultrafast spectroscopic techniques across the electronic and vibrational domains to demonstrate the light-induced ultrafast ESIPT and structural dynamics of the BBM molecules in different solvents. Building upon all the experimental and calculation results, we can draw a schematic diagram of the potential energy surface summarizing the photo-induced structural dynamics observed in BBM (see Figure 5). Upon vertical excitation of BBM-enol to its excited state BBM-enol*, it undergoes ESIPT in one HBI half of BBM, resulting in the formation of the deprotonated BBM-keto* state (300 fs time constant). This is followed by the decay of BBM-keto* to ground state BBM-keto via 438 nm fluorescence (with a lifetime of 1.3 ns), and simultaneously planarization through variation in dihedral angle Θ between the two HBI halves, resulting in dynamic fluorescence redshift to 445 nm. This work demonstrates that FSRS, after successful assignment by quantum chemical calculation, especially when combined with the time-resolved electronic spectroscopies, is a powerful method for uncovering the ultrafast and small structural changes of the chromophore under the effect of the different solvent environments.

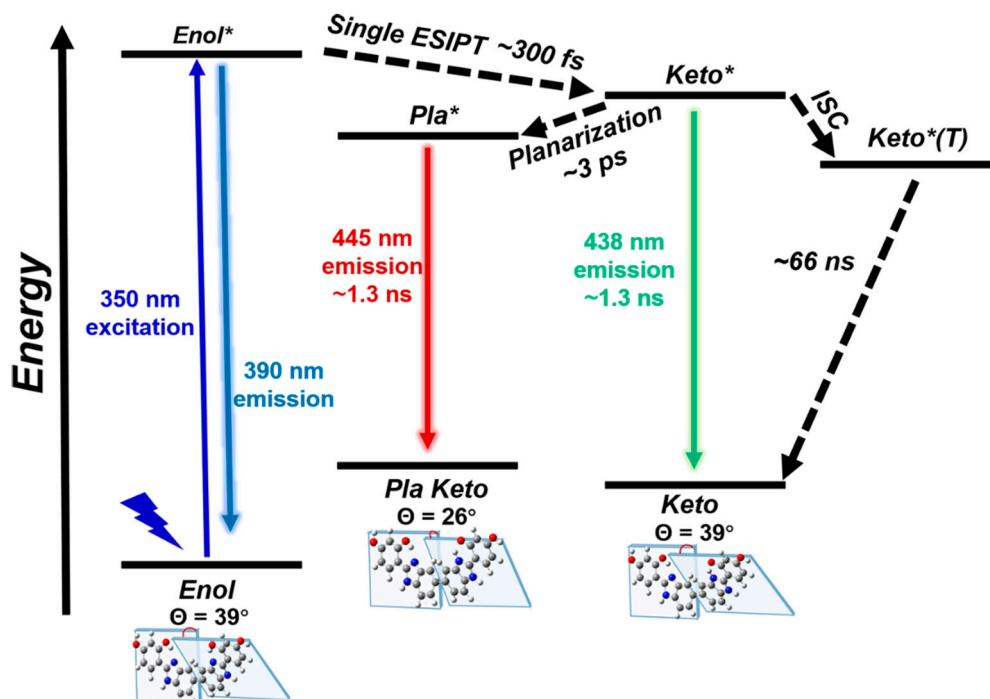


Figure 5. Schematic representation of photodynamic of BBM in DMSO. Pla (planarized), ESIPT (excited state intramolecular proton transfer), ISC (intersystem crossing).

Supplementary Materials: The following supporting information can be downloaded at the website of this paper posted on Preprints.org.

Author Contributions: designed and supervised the project, W.L., T.W.; performed spectroscopic measurements with data analysis, J.X., R.Z. and Z.W., J.J.; quantum chemical calculations, Y.H., Y.R.; data interpretation, J.X., J.J.; synthesizing sample, S.H.; wrote the manuscript, J.X., W.L.; funding acquisition, W.L., Y.H.

Funding: The research was funded by the Natural Science Foundation of Shanghai (20ZR1436300); National Natural Science Foundation of China (Nos.21872094); Double First-Class Initiative Fund of ShanghaiTech University; ShanghaiTech Start-up Funding (F-0201-16-006), and the Foundation of STU and SIOM Joint Laboratory for Superintense Lasers and the Applications.

Data Availability Statement: Not applicable.

Acknowledgments: H. Y. F. acknowledges the HPC Platform of ShanghaiTech University Library and Information Services for use of their supercomputer facilities.

Conflicts of Interest: The authors declare no conflict of interest.

References

1. Henary, M. M.; Wu, Y.; Fahrni, C. J., Zinc(II)-selective ratiometric fluorescent sensors based on inhibition of excited-state intramolecular proton transfer. *Chem. Eur. J.* **2004**, *10* (12), 3015-25.
2. Xu, Y.; Liu, Q.; Dou, B.; Wright, B.; Wang, J.; Pang, Y., Zn²⁺ binding-enabled excited state intramolecular proton transfer: a step toward new near-infrared fluorescent probes for imaging applications. *Adv. Healthcare Mater.* **2012**, *1* (4), 485-92.
3. Kwon, J. E.; Lee, S.; You, Y.; Baek, K. H.; Ohkubo, K.; Cho, J.; Fukuzumi, S.; Shin, I.; Park, S. Y.; Nam, W., Fluorescent zinc sensor with minimized proton-induced interferences: photophysical mechanism for fluorescence turn-on response and detection of endogenous free zinc ions. *Inorg. Chem.* **2012**, *51* (16), 8760-74.
4. Akutsu, K.; Mori, S.; Shinmei, K.; Iwase, H.; Nakano, Y.; Fujii, Y., Investigation of substitution effect on fluorescence properties of Zn²⁺ elective ratiometric fluorescent compounds: 2-(2'-Hydroxyphenyl)benzimidazole derivatives. *Talanta* **2016**, *146*, 575-84.

5. Bag, R.; Sikdar, Y.; Sahu, S.; Das Mukhopadhyay, C.; Drew, M. G. B.; Goswami, S., Benzimidazole based ESIPT active chemosensors enable nano-molar detection of Cu²⁺ in 90% aqueous solution, MCF-7 cells, and plants. *J. Photochem. Photobiol., A* **2022**, 431.
6. Barbatti, M.; Aquino, A. J.; Lischka, H.; Schriever, C.; Lochbrunner, S.; Riedle, E., Ultrafast internal conversion pathway and mechanism in 2-(2'-hydroxyphenyl)benzothiazole: a case study for excited-state intramolecular proton transfer systems. *PCCP* **2009**, 11 (9), 1406-15.
7. de Vivie-Riedle, R.; De Waele, V.; Kurtz, L.; Riedle, E., Ultrafast excited-state proton transfer of 2-(2'-hydroxyphenyl)benzothiazole: Theoretical analysis of the skeletal deformations and the active vibrational modes. *J. Phys. Chem. A* **2003**, 107 (49), 10591-10599.
8. Lochbrunner, S.; Wurzer, A. J.; Riedle, E., Ultrafast excited-state proton transfer and subsequent coherent skeletal motion of 2-(2'-hydroxyphenyl)benzothiazole. *J. Chem. Phys.* **2000**, 112 (24), 10699-10702.
9. Aly, S. M.; Usman, A.; AlZayer, M.; Hamdi, G. A.; Alarousu, E.; Mohammed, O. F., Solvent-dependent excited-state hydrogen transfer and intersystem crossing in 2-(2'-hydroxyphenyl)-benzothiazole. *J. Phys. Chem. B* **2015**, 119 (6), 2596-603.
10. Wang, H.; Zhang, H.; Abou-Zied, O. K.; Yu, C.; Romesberg, F. E.; Glasbeek, M., Femtosecond fluorescence upconversion studies of excited-state proton-transfer dynamics in 2-(2'-hydroxyphenyl)benzoxazole (HBO) in liquid solution and DNA. *Chem. Phys. Lett.* **2003**, 367 (5-6), 599-608.
11. Kim, C. H.; Park, J.; Seo, J.; Park, S. Y.; Joo, T., Excited State Intramolecular Proton Transfer and Charge Transfer Dynamics of a 2-(2'-Hydroxyphenyl)benzoxazole Derivative in Solution. *J. Phys. Chem. A* **2010**, 114 (18), 5618-5629.
12. Vazquez, S. R.; Rodriguez, M. C. R.; Mosquera, M.; Rodriguez-Prieto, F., Excited-state intramolecular proton transfer in 2-(3'-hydroxy-2'-pyridyl)benzoxazole. Evidence of coupled proton and charge transfer in the excited state of some o-hydroxyarylbenzoxazoles. *J. Phys. Chem. A* **2007**, 111 (10), 1814-1826.
13. Vazquez, S. R.; Rodriguez, M. C. R.; Mosquera, M.; Rodriguez-Prieto, F., Rotamerism, tautomerism, and excited-state intramolecular proton transfer in 2-(4'-N,N-diethylamino-2'-hydroxyphenyl)benzimidazoles: Novel benzimidazoles undergoing excited-state intramolecular coupled proton and charge transfer. *J. Phys. Chem. A* **2008**, 112 (3), 376-387.
14. Frey, W.; Laermer, F.; Elsaesser, T., Femtosecond Studies of Excited-State Proton and Deuterium Transfer in Benzothiazole Compounds. *J. Phys. Chem.* **1991**, 95 (25), 10391-10395.
15. Irvani, M.; Omidyan, R., Photochromism of 2-(2-Hydroxyphenyl) Benzothiazole (HBT) and Its Derivatives: A Theoretical Study. *J. Phys. Chem. A* **2018**, 122 (12), 3182-3189.
16. Pijeu, S.; Foster, D.; Hohenstein, E. G., Excited-State Dynamics of 2-(2'-Hydroxyphenyl)benzothiazole: Ultrafast Proton Transfer and Internal Conversion. *J. Phys. Chem. A* **2017**, 121 (24), 4595-4605.
17. Mohammed, O. F.; Luber, S.; Batista, V. S.; Nibbering, E. T., Ultrafast branching of reaction pathways in 2-(2'-hydroxyphenyl)benzothiazole in polar acetonitrile solution. *J. Phys. Chem. A* **2011**, 115 (26), 7550-8.
18. Alarcos, N.; Gutierrez, M.; Liras, M.; Sanchez, F.; Douhal, A., An abnormally slow proton transfer reaction in a simple HBO derivative due to ultrafast intramolecular-charge transfer events. *PCCP* **2015**, 17 (25), 16257-69.
19. Kayal, S.; Roy, K.; Lakshmana, Y. A.; Umapathy, S., Probing the effect of solvation on photoexcited 2-(2'-hydroxyphenyl)benzothiazole via ultrafast Raman loss spectroscopic studies. *J. Chem. Phys.* **2018**, 149 (4), 044310.
20. Wei, J.; Wu, Y.; Pu, R.; Shi, L.; Jiang, J.; Du, J.; Guo, Z.; Huang, Y.; Liu, W., Tracking Ultrafast Structural Dynamics in a Dual-Emission Anti-Kasha-Active Fluorophore Using Femtosecond Stimulated Raman Spectroscopy. *J. Phys. Chem. Lett.* **2021**, 12 (18), 4466-4473.
21. Xu, W.; Wei, L.; Wang, Z.; Zhu, R.; Jiang, J.; Liu, H.; Du, J.; Weng, T.-C.; Zhang, Y.-B.; Huang, Y.; Liu, W., Tracking Ultrafast Fluorescence Switch-On and Color-Tuned Dynamics in Acceptor-Donor-Acceptor Chromophore. *J. Phys. Chem. B* **2021**, 125 (38), 10796-10804.
22. Zhang, W.; Xu, W.; Zhang, G.; Kong, J.; Niu, X.; Chan, J. M. W.; Liu, W.; Xia, A., Direct Tracking Excited-State Intramolecular Charge Redistribution of Acceptor-Donor-Acceptor Molecule by Means of Femtosecond Stimulated Raman Spectroscopy. *J. Phys. Chem. B* **2021**, 125 (17), 4456-4464.
23. Liu, W.; Han, F.; Smith, C.; Fang, C., Ultrafast conformational dynamics of pyranine during excited state proton transfer in aqueous solution revealed by femtosecond stimulated Raman spectroscopy. *J. Phys. Chem. B* **2012**, 116 (35), 10535-50.
24. Fang, C.; Tang, L.; Oscar, B. G.; Chen, C., Capturing Structural Snapshots during Photochemical Reactions with Ultrafast Raman Spectroscopy: From Materials Transformation to Biosensor Responses. *J. Phys. Chem. Lett.* **2018**, 9 (12), 3253-3263.
25. Liu, W.; Tang, L.; Oscar, B. G.; Wang, Y.; Chen, C.; Fang, C., Tracking Ultrafast Vibrational Cooling during Excited-State Proton Transfer Reaction with Anti-Stokes and Stokes Femtosecond Stimulated Raman Spectroscopy. *J. Phys. Chem. Lett.* **2017**, 8 (5), 997-1003.

26. Hao, X.; Han, S.; Zhu, J.; Hu, Y.; Chang, L. Y.; Pao, C. W.; Chen, J. L.; Chen, J. M.; Haw, S. C., A bis-benzimidazole PMO ratiometric fluorescence sensor exhibiting AIEE and ESIPT for sensitive detection of Cu²⁺. *RSC Adv.* **2019**, 9 (24), 13567-13575.
27. G.J.Woolfe; M.Melzig; S.Schneider; F.Dörr, The role of tautomeric and rotameric species in the photophysics of 2-(2'-hydroxyphenyl)benzoxazole. *Chemical Physics* **1983**, 77, 213-221.
28. Abou-Zied, O. K.; Jimenez, R.; Thompson, E. H. Z.; Millar, D. P.; Romesberg, F. E., Solvent-Dependent Photoinduced Tautomerization of 2-(2'-Hydroxyphenyl)benzoxazole. *J. Phys. Chem. A* **2002**, 106, 3665-3672.
29. Chou, P. T.; Studer, S. L.; Martinez, M. L., Studies of the Triplet-State of 2-(2'-Hydroxyphenyl)Benzothiazole. *Chem. Phys. Lett.* **1991**, 178 (4), 393-398.
30. Ohshima, A.; Momotake, A.; Nagahata, R.; Arai, T., Enhancement of the large Stokes-shifted fluorescence emission from the 2-(2'-hydroxyphenyl)benzoxazole core in a dendrimer. *J. Phys. Chem. A* **2005**, 109 (43), 9731-9736.
31. Horng, M. L.; Gardecki, J. A.; Maroncelli, M., Rotational dynamics of coumarin 153: Time-dependent friction, dielectric friction, and other nonhydrodynamic effects. *J. Phys. Chem. A* **1997**, 101 (6), 1030-1047.
32. Horng, M. L.; Gardecki, J. A.; Papazyan, A.; Maroncelli, M., Subpicosecond Measurements of Polar Solvation Dynamics - Coumarin-153 Revisited. *J. Phys. Chem.* **1995**, 99 (48), 17311-17337.
33. Maus, M.; Rettig, W.; Bonafoux, D.; Lapouyade, R., Photoinduced intramolecular charge transfer in a series of differently twisted donor - Acceptor biphenyls as revealed by fluorescence. *J. Phys. Chem. A* **1999**, 103 (18), 3388-3401.
34. Chen, W.; Chen, C. L.; Zhang, Z.; Chen, Y. A.; Chao, W. C.; Su, J.; Tian, H.; Chou, P. T., Snapshotting the Excited-State Planarization of Chemically Locked N,N'-Disubstituted Dihydrodibenzo[a,c]phenazines. *J. Am. Chem. Soc.* **2017**, 139 (4), 1636-1644.
35. Chen, D. G.; Chen, Y.; Wu, C. H.; Chen, Y. A.; Chen, M. C.; Lin, J. A.; Huang, C. Y.; Su, J.; Tian, H.; Chou, P. T., Phenothiazine Scope: Steric Strain Induced Planarization and Excimer Formation. *Angew. Chem. Int. Ed.* **2019**, 58 (38), 13297-13301.
36. Guo, Y.; Abeywickrama, C. S.; Huo, D.; Kong, J.; Tao, M.; Xia, A.; Pang, Y.; Wan, Y., Solvation Controlled Excited-State Planarization in a Push-Pull Pyrene Dye. *J. Phys. Chem. C* **2020**, 124 (16), 8550-8560.
37. Fang, C.; Frontiera, R. R.; Tran, R.; Mathies, R. A., Mapping GFP structure evolution during proton transfer with femtosecond Raman spectroscopy. *Nature* **2009**, 462 (7270), 200-U74.
38. Liu, W. M.; Wang, Y. L.; Tang, L. T.; Oscar, B. G.; Zhu, L. D.; Fang, C., Panoramic portrait of primary molecular events preceding excited state proton transfer in water. *Chem. Sci.* **2016**, 7 (8), 5484-5494.
39. Miertuš, S.; Scrocco, E.; J. Tomasi, C., <Electrostatic interaction of a solute with a continuum. A direct utilizaion of AB initio molecular potentials for the prevision of solvent effects. *Chem. Phys.* **1981**, 55, 117-129.
40. Miertuš, S.; Tomasi, J., Approximate evaluations of the electrostatic free energy and internal energy changes in solution processes. *Chem. Phys.* **1982**, 65, 239-245.
41. Lee, C.; Yang, W.; Parr, R. G., Development of the Colle-Salvetti correlation-energy formula into a functional of the electron density. *Phys. Rev. B* **1988**, 37 (2), 785-789.
42. Becke, A. D., Perspective on "Density functional thermochemistry. III. The role of exact exchange". *J. Chem. Phys.* **1993**, 98 (3-4), 5648-5652.
43. Pascual-ahuir, J. L.; Silla, E.; Tuñón, I., GEPOL: An improved description of molecular surfaces. III. A new algorithm for the computation of a solvent-excluding surface. *J. Comput. Chem.* **1994**, 15 (10), 1127-1138.
44. Frisch, M.; Trucks, G.; Schlegel, H. B.; Scuseria, G. E.; Robb, M. A.; Cheeseman, J. R.; Scalmani, G.; Barone, V.; Mennucci, B.; Petersson, G., gaussian 09, Revision d. 01, Gaussian, Inc., Wallingford CT **2009**, 201.

Disclaimer/Publisher's Note: The statements, opinions and data contained in all publications are solely those of the individual author(s) and contributor(s) and not of MDPI and/or the editor(s). MDPI and/or the editor(s) disclaim responsibility for any injury to people or property resulting from any ideas, methods, instructions or products referred to in the content.